# Long and short-term changes of Keplerian elements and correction coefficients of GPS satellites

Kamil Maciuk

AGH University of Science and Technology, al. Mickiewicza 30 30-059 Kraków, Poland

[E-mail: maciuk@agh.edu.pl]

In satellite geodesy, the motion of artificial satellites has a crucial importance and the satellite's position is the core point in the geodetic network. The simplicity of the broadcast ephemeris model directly determines the rate and efficiency of real-time navigation and positioning. GNSS broadcast message is transmitted in ECEF system either (GLONASS) or are Keplerian-like orbital elements (GPS, BeiDou, Galileo). The main aim of this paper is to describe the magnitude of Keplerian elements and correction coefficients of the navigational satellite changes based on a GPS satellite. The author examines six Keplerian elements and six correction coefficients for three different intervals: 2-hour, 1-day and 5-day intervals for periods of 9 days, a year and 10 years respectively. The analysis shows the varying behaviour of the time-series of the analysed components on the basis of the on-board GPS message, both random-like and repetitive (seasonal) trajectory time series.

[**Keywords**: Ephemeris, GPS, Keplerian orbital elements, Orbit, Orbital elements]

## Introduction

The GPS broadcast ephemeris is the basis of satellite navigation and positioning[1,2]. GPS ephemeris are forecast, predicted or extrapolated satellite orbit data, which are transmitted to the receiver from the satellite via a navigation message[3]. The GPS navigational message is available in real-time, therefore it constitutes the essence of standalone positioning as well of RTK measurements, which are today in use in various areas, e.g. geodesy[4–6], crustal deformations analysis[7], spatial analysis[8,9] or thermography[10,11]. GPS broadcasts a message as Keplerian ephemeris parameters[12]. Keplerian motion is called simplified satellite orbiting and the problem is called the two-body problem. An artificial Earth satellite (AES) moves in a central force field and its mass is negligibly small compared to the mass of the Earth ($M$). According to Newton's second law of motion[13], satellite motion is described as[14]:

$$\ddot{r} = -\frac{\mu}{r^2}\frac{r}{r} \qquad \dots (1)$$

where $\ddot{r}$ is the acceleration of the motion (second order differentiation of vector $r$ with respect to time) and $\mu$ (= $GM$, $G$ is the universal gravitational constant) is the Earth's so-called gravitational potential. Equation (1) describes the motion of the satellite in the gravity field of the central body $M$, on the assumption of its symmetry (sphere). Acceleration

magnitude depends on the quotient of the statement $1/r^2$ — it is inversely proportional to the distance between the central body (Earth) and the satellite. The transformation of equation (1) to the general form of a two-body problem without taking into consideration the influence of the satellite on the central body $M$ (the so-called limited case of the two-body problem) and with assumption of the position consistency of the $M$ body against the origin of the coordinate system leads to the equation:

$$\ddot{r} + \frac{\mu}{r^2}\frac{r}{r} = 0 \qquad \dots (2)$$

Equation (2) is a second order differential equation. The geometric centre of the central body overlap with the origin of the coordinate system vector's $r$ coordinates will be defined as $x, y, z$ and the vector of differential equation (2) may be substituted with three scalar second order differential equations:

$$\ddot{x} + \frac{\mu}{r^3}x = 0$$

$$\ddot{z} + \frac{\mu}{r^3}z = 0$$

$$\ddot{y} + \frac{\mu}{r^3}y = 0 \qquad \dots (3)$$

where $r = \sqrt{x^2 + y^2 + z^2}$. The analytical solution of equation (2) leads to the Keplerian motion defined by six parameters[15] presented in Table 1.

Table 1 — Keplerian orbital parameters[16].

| Parameter | Notation |
|---|---|
| $a$ | semi-major axis of orbital ellipse |
| $e$ | numerical eccentricity of ellipse |
| $\tau$ | epoch of perigee passage |
| $\omega$ | argument of perigee |
| $i$ | inclination of orbital plane |
| $\Omega$ | right ascension of ascending node |

Table 2 — Summary of approximate perturbing forces for GPS satellite[23].

| Source | Maximum perturbing acceleration [m/s²] | Maximum excursion growth in one hour [m/s²] |
|---|---|---|
| Earth-mass attraction | $5.65 \cdot 10^{-1}$ | — |
| Second zonal harmonic | $5.3 \cdot 10^{-5}$ | 300 |
| Lunar gravity | $5.5 \cdot 10^{-6}$ | 40 |
| Solar gravity | $3 \cdot 10^{-6}$ | 20 |
| Fourth zonal harmonic | $10^{-7}$ | 0.6 |
| Solar radiation pressure | $10^{-7}$ | 0.6 |
| Gravity anomalies | $10^{-8}$ | 0.06 |
| All other forces | $10^{-8}$ | 0.06 |

The first two parameters ($a$ and $e$) define the size and shape of elliptical orbits. The argument of perigee ($\omega$) defines the location of the body against the equator plane (Fig. 1). The orientation of the circulating body against the equator plane defines the inclination angle ($i$) and the right ascension of the ascending node ($\Omega$). The above parameters define others, such as altitude or orbital period (half a sidereal day)[17]. Keplerian elements can be characterised by annual, semi-annual or draconitic courses[18].

Keplerian parameters can be divided into two groups[20]: dynamical constants ($a$, $e$, $\tau$) and spatial orientation of the angles of eclipse ($\omega$, $i$, $\Omega$). Perturbation forces acting on the orbital motion of the AES cause a difference between the actual position of the satellite and the position calculated on the basis of Keplerian elements[21], therefore this position cannot be described by equation (2). Therefore, equations of motion can be described as[14,22]:

$$\ddot{r} = -\mu \frac{r}{r^3} + a(t; r, \dot{r}, d_1, d_2, \ldots, d_m) \qquad \ldots (4)$$

where:

$\ddot{r}$ — geocentric acceleration vector of the satellite
$a$ — perturbing acceleration
$r$ — geocentric position vector of the satellite
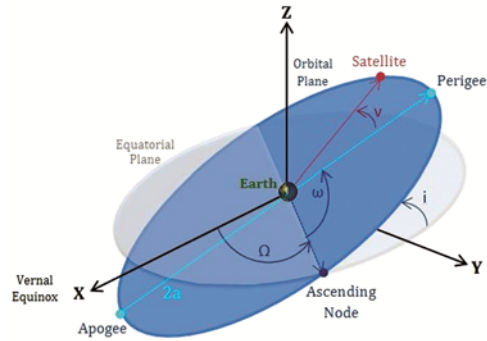$\dot{r}$ — geocentric velocity vector of the satellite



Fig. 1 — The Keplerian elements of an elliptical orbit[19].

$d_j$ — dynamical parameters, $j = 1 \ldots m$

The first element in equation (4) is the force exerted by the central body, whereas vector $\alpha$ represents the sum of all perturbing accelerations affecting the AES's motion. Satellite perturbing forces may be described by a series of instantaneous Keplerian orbits deviates from true trajectory. The set of orbital elements assigned to the satellite vector of state on each epoch $t$ may be described by the equation:

$$\{r(t), \dot{r}(t)\} \leftrightarrow \{a(t), e(t), t(i), \Omega(t), \omega(t), \tau(t)\} \qquad \ldots (5)$$

These elements are osculatory to the real orbit on a particular epoch $t^{22}$. Accelerations caused by the gravity of other celestial bodies and forces not related to gravitational forces have an influence on the movement of the satellite. The role of these forces is negligibly small compared to the accuracy of the determined position. Table 2 presents the greatest perturbing forces acting on the AES:

The second zonal harmonic arising from the Earth's flatness is the biggest perturbing force. The influence of the Moon and the Sun is one order of magnitude smaller. The rest of the perturbing forces in the navigational satellite motion computation due to their insignificant size may be ignored.

**Materials and methods**

Two different approaches are followed in computing earth-centred, earth-fixed (ECEF) coordinates from GNSS broadcast orbits. Based on Keplerian elements transmitted in the navigational message, ECEF coordinates are computed as an analytical function with a 2-hour update rate of broadcast data[14]. This approach is adopted by GPS, Galileo, BeiDou, IRNSS and QZSS[24,25]. The second approach is based on the numerical integration of nine elements of the vector of state (three positions,

velocities and accelerations). The vector of state is transmitted every 30 minutes and is in use in GLONASS, GAGAN and EGNOS[25]. In this work, the author analysed changes of data transmitted in GPS broadcast messages (Table 3).

Table 3 — Ephemeris data definitions[26].

| Notation | Data description |
|---|---|
| $M_0$ | Mean anomaly of reference time |
| $\Delta n$ | Mean motion difference from computed value |
| $e$ | Eccentricity |
| $\sqrt{a}$ | Square root of the semi-major axis |
| $\Omega_0$ | Longitude of ascending node of orbit plane at weekly epoch |
| $i_0$ | Inclination angle at reference time |
| $\omega$ | Argument of perigee |
| $\dot{\Omega}$ | Rate of right ascension |
| idot | Rate of inclination angle |
| $C_{uc}$ | Amplitude of the cosine harmonic correction term to the argument of latitude |
| $C_{us}$ | Amplitude of the sine harmonic correction term to the argument of latitude |
| $C_{rc}$ | Amplitude of the cosine harmonic correction term to the orbit radius |
| $C_{rs}$ | Amplitude of the sine harmonic correction term to the orbit radius |
| $C_{ic}$ | Amplitude of the cosine harmonic correction term to the angle of inclination |
| $C_{is}$ | Amplitude of the sine harmonic correction term to the angle of inclination |
| $t_{OE}$ | Reference time ephemeris |
| IODE | Issue of data (ephemeris) |

The parameters presented in Table 3 allow the coordinates of the satellite in the ECEF coordinate system to be computed[27], and the details of the computation have already been widely described in the literature, e.g. Beutler *et al.*[15], Ogaza[28], Li[29], and Hugentobler & Montenbruck[30].

**Results and discussion**

In this paper, six elements of Keplerian orbit and six correction element changes were analysed. These values were collected from GPS navigational messages between 1064 and 1616 GPS week (years 2000-2010, 552 weeks, almost 10.6 years) of GPS satellite PRN 10. An analysis was conducted for three different periods:

— 9 days with a 2-hour interval (1 - 9 Sep 2010)
— 1 year with a 1-day int. (Jan - Dec 2010)
— 10 years with a 5-day int. (May 2000 - Dec 2010)

Figure 2 presents the behaviour of Keplerian elements in 2-hour intervals with 9-day coverage. Short-periodic perturbations dominate the semi-major axis $a$, eccentricity $e$ and argument of perigee $\omega$ with a polynomial trend for the entire analysed period. In the case of the mean anomaly of reference time $M_0$, there is clearly seen a repeatable, sawtooth pattern with a close to 12-hour long period (half a sidereal day – GPS satellite evolution period). An analysis of the year-long time-series with a 1-day interval shows similar, periodical fluctuations for the same parameters
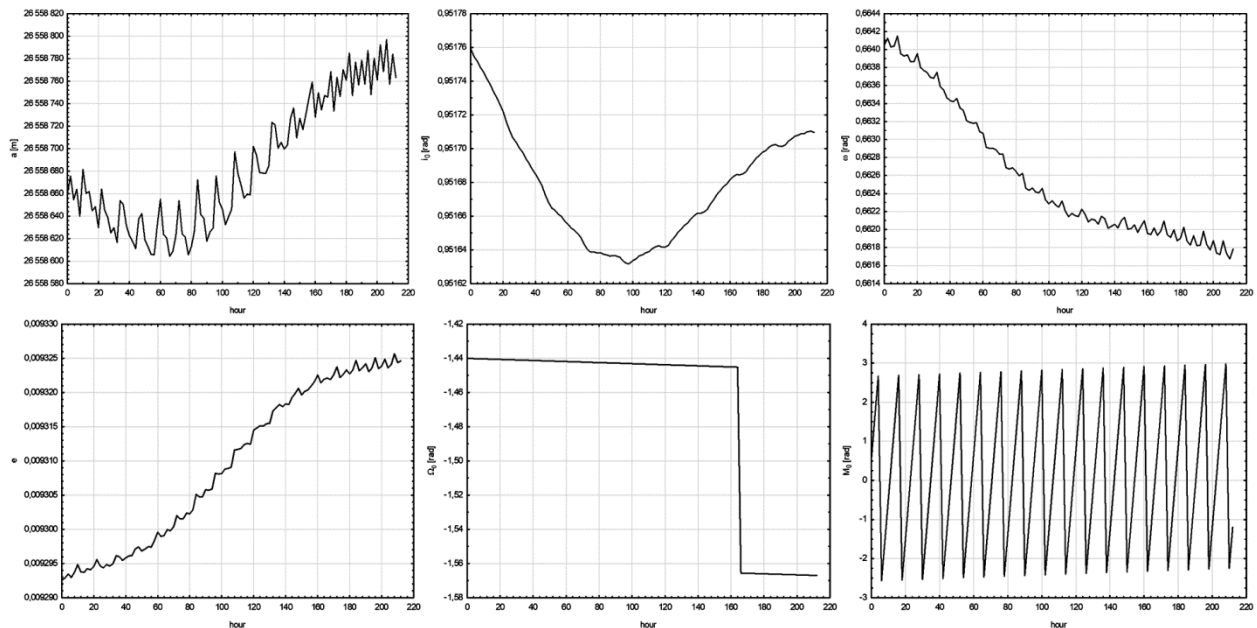


Fig. 2 — Time-series of Keplerian elements in 2 hours intervals.

presented in Figure 3. In the case of the semi-major axis and longitude of the ascending node $\Omega_0$, the patterns have a linear trend with single pitches. In the case of three parameters $(i, \omega, e)$, there is a long-term polynomial trend and the mean anomaly of reference time $M_0$ pattern has a random changes ranging from -3 to 3. Figure 4 presents the behaviour of Keplerian elements in 5-day intervals covering 10 years of observations. The time-series of three elements $(i, \omega, e)$

present polynomial behaviour with imposed sinusoidal fluctuations with annual $(\omega, e)$ and semi-annual $(i)$ period oscillations. In the case of the semi-major axis $a$ and longitude of the ascending node $\Omega_0$, the time-series demonstrates a sawtooth graph plot with an annual period. In the case of the mean anomaly of reference time $M_0$, the graph oscillates within a range of -3 to 3 with a random-like, close to annual period. The behaviour of correction coefficients is presented in
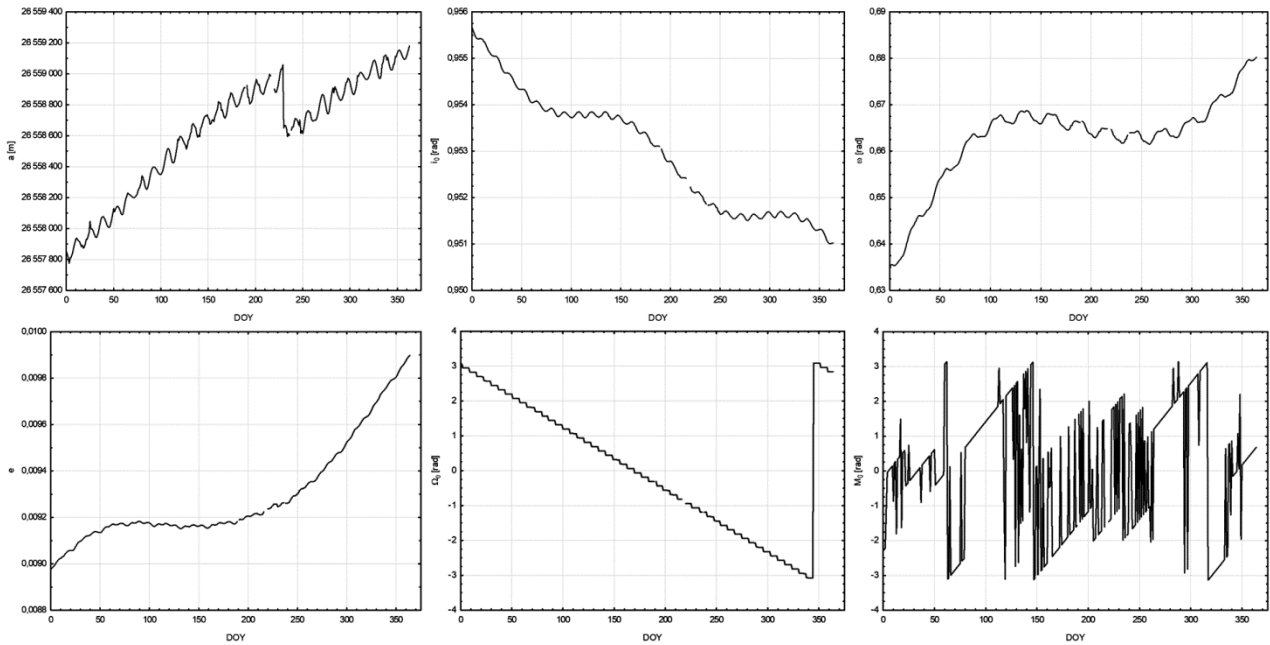


Fig. 3 — Time-series of Keplerian elements in daily intervals
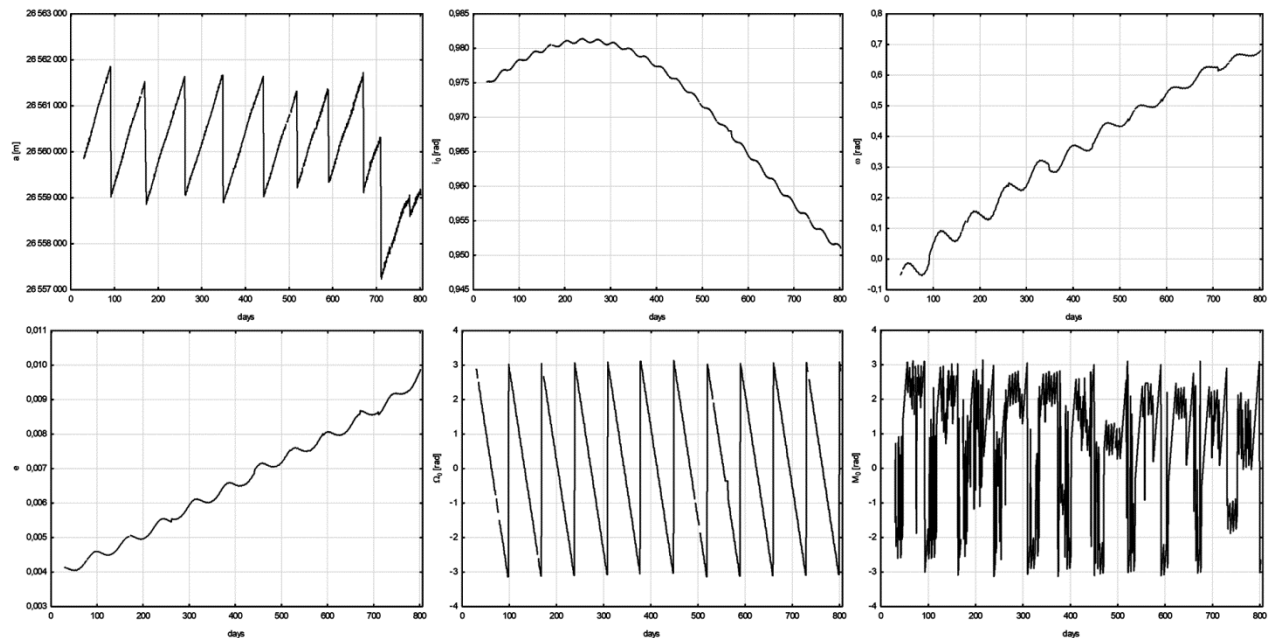


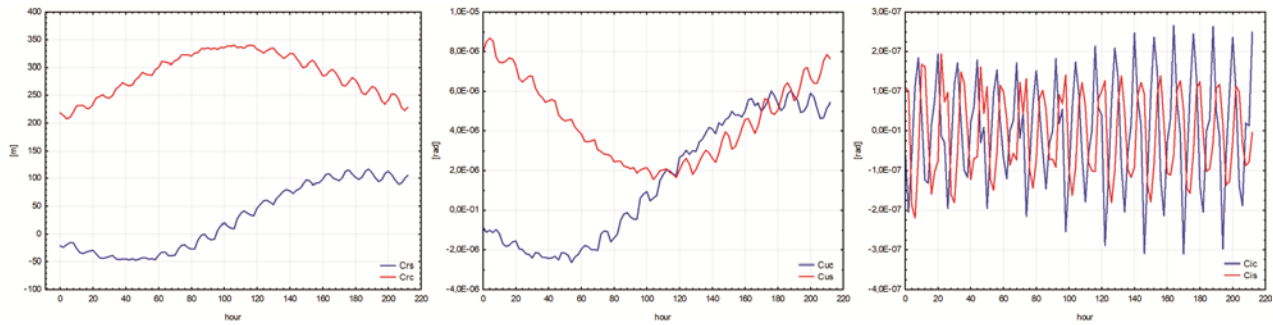Fig. 4 — Time-series of Keplerian elements in 5 days intervals

Fig. 5 — Time-series of corrections coefficients values in 2 hours intervals
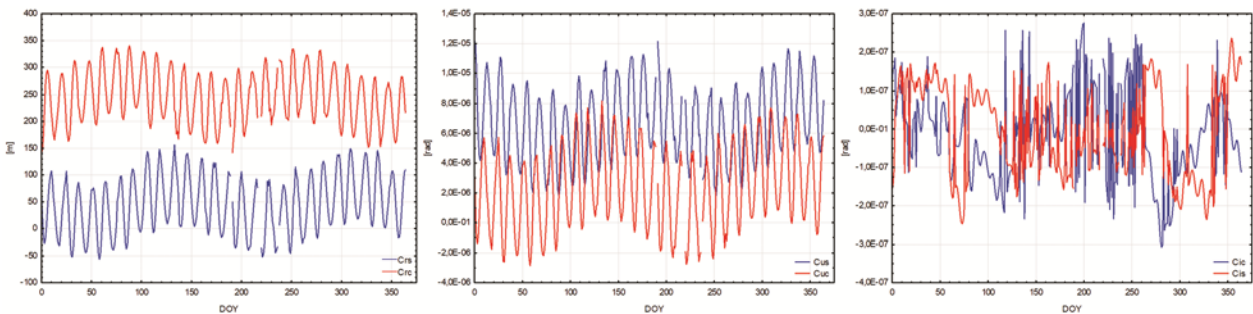


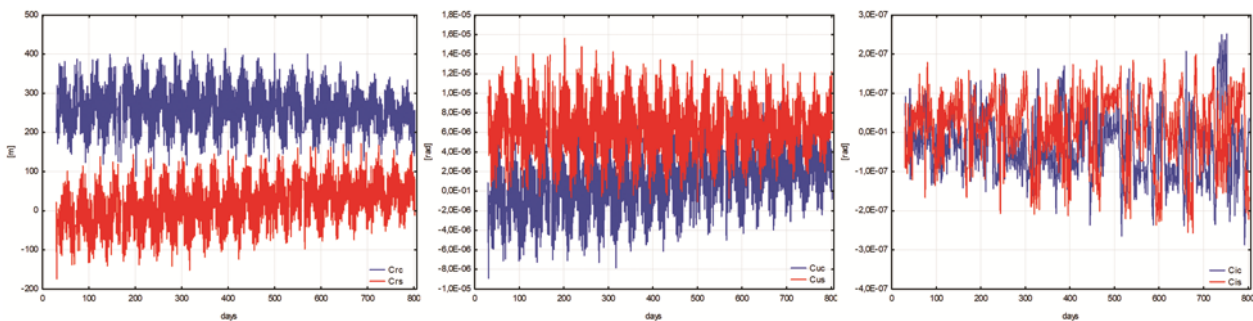Fig. 6 — Time-series of corrections coefficients values in a daily intervals



Fig. 7 — Time-series of corrections coefficients values in 5 days intervals

Figures 5-7. Each coefficient has periodical sinusoidal fluctuations with half a sidereal day. An analysis of annual graphs of four coefficient $C_{rc}, C_{rs}, C_{us}, C_{uc}$ time series presents periodical fluctuations with a nearly 13.5-day period. The coefficients $C_{ic}, C_{is}$ time series present a pseudorandom noise course both for the year period (1-day interval) and for 10 years (5-day interval). The coefficients $C_{rc}, C_{rs}, C_{us}, C_{uc}$ time series in the 10-year period have a sinusoidal course with a 175-day period, which is very close to half of a draconitic year.

## Conclusion

The paper discusses the orbits of GPS satellites and the author looks at the Keplerian element changes based on the navigational message. There is an analysis of six Keplerian elements and six correction coefficient time series in three different intervals: 2 hours, 1 day and 5 days. The analysis shows the varying behaviour of the analysed time series both in short- and long-time periods, the majority of which is characterised by seasonal, repetitive changes. Short-term sinusoidal fluctuations are imposed on long-term close to annual, semi-annual and even draconitic periods, which can be extrapolated and whose values may be anticipated.

## Acknowledgment

## References

1   Wang, A., Chen, J. & Wang, J., Precision Analysis of CNAV Broadcast Ephemeris and Its Impact on the User Positioning. In: *China Satellite Navigation Conference (CSNC) 2017 Proceedings*: Volume I edited by Sun, J., Liu, J., Yang, Y., Fan, S. & Yu, W., (Springer Singapore) 2017, 431–440.

2    Maciuk, K. & Lewińska, P., High-Rate Monitoring of Satellite Clocks Using Two Methods of Averaging Time. *Remote Sens.*, 11 (2019) 2754. doi:10.3390/rs11232754

3    Xu, G. & Xu, Y., In: *GPS: Theory, Algorithms and Applications*, (Springer Berlin Heidelberg New York) 2013, pp. 353. ISBN: 978-3-540-72714-9

4    Krzyżek, R., Uchański, J. & Falkowski, P., The SWSC Compilation Algorithm enhancing the reliability and accuracy of determining rectangular co-ordinates of corners of building structures with photogrammetric method. *Measurement,* 110 (2017) 154–165. doi:10.1016/j.measurement.2017.06.016

5    Maciuk, K., GPS-only, GLONASS-only and Combined GPS+GLONASS Absolute Positioning under Different Sky View Conditions. *Teh. Vjesn. - Tech. Gaz.,* 25 (2018). doi:10.17559/TV-20170411124329

6    Borowski, L. & Banasik, P., The conversion of heights of the benchmarks of the detailed vertical reference network into the PL-EVRF 2007-NH frame. *Reports Geod. Geoinformatics,* 109 (2020) 1–7. doi:10.2478/rgg-2020-0001

7    Maciuk, K., The study of seasonal changes of permanent stations coordinates based on weekly EPN solutions. *Artif. Satell.*, 51 (2016) 1–18. doi: 10.1515/arsa-2016-0001

8    Benduch, P., Pęska-Siwik, A. & Hanus, P., Problematic aspects of registering ecological land-use in the Real Estate Cadastre. *E3S Web Conf.,* 86 (2019) 00007. doi:10.1051/e3sconf/20198600007

9    Hanus, P., Pęska-Siwik, A., Benduch, P. & Szewczyk, R., Comprehensive Assessment of the Quality of Spatial Data in Records of Parcel Boundaries. *Measurement,* (2020) pp. 107665. doi:10.1016/j.measurement.2020.107665

10   Lewińska, P., Matula, R. & Dyczko, A., Integration of Thermal Digital 3D Model and a MASW (Multichannel Analysis of Surface Wave) as a Means of Improving Monitoring of Spoil Tip Stability. In: *2017 Baltic Geodetic Congress (BGC Geomatics)* (2017) 232–236. doi:10.1109/BGC.Geomatics.2017.29

11   Lewińska, P. & Dyczko, A., Thermal digital terrain model of a coal spoil tip – a way of improving monitoring and early diagnostics of potential spontaneous combustion areas. *J. Ecol. Eng.,* 17 (2016) 170–179. doi:10.12911/22998993/64605

12   Heng, L., Gao, G. X., Walter, T. & Enge, P., Statistical Characterization of GLONASS Broadcast Clock Errors and Signal-In-Space Errors. *Proc. Int. Tech. Meet. Inst. Navig.,* (2012) 1697–1707. ISBN:9781618399205

13   Jo, J.-H., Park, I.-K., Choe, N.-M. & Choi, M. S., The Comparison of the Classical Keplerian Orbit Elements, Non-Singular Orbital Elements (Equinoctial Elements), and the Cartesian State Variables in Lagrange Planetary Equations with J 2 Perturbation: Part I. *J. Astron. Sp. Sci.,* 28 (2011) 37–54. doi:10.5140/JASS.2011.28.1.037

14   Maciuk, K., Different approaches in GLONASS orbit computation from broadcast ephemeris. *Geod. Vestn.*, 60 (2016) 455–466. doi:10.15292/geodetski-vestnik.2016.03.455-466

15   Beutler, G., Weber, R., Hugentobler, U., Rothacher, M. & Verdun, A., GPS satellite orbits. In: *GPS for Geodesy*, edited by Kleusberg, A., Teunissen, P., (Springer Berlin Heidelberg New York) 1996, 37–101. ISBN:978-3-642-72011-6

16   Hofmann-Wellenhof, B., Lichtenegger, H. & Collins, J., Satellite orbits. In: *Global Positioning System*, edited by Hofmann-Wellenhof, B., Lichtenegger, H., Collins, J., (Springer Berlin Heidelberg New York) (1997) 41–72. ISBN:978-3-7091-6199-9

17   Bock, Y., Nikolaidis, R. M., de Jonge, P. J. & Bevis, M., Instantaneous geodetic positioning at medium distances with the Global Positioning System. *J. Geophys. Res.,* 105 (2000) 28223. doi:10.1029/2000JB900268

18   Melachroinos, S. A. *et al*. The effect of seasonal and long-period geopotential variations on the GPS orbits. *GPS Solut.,* 18 (2014) 497–507. doi:10.1007/s10291-013-0346-4

19   https://www.gsc-europa.eu/system-service-status/orbital-and-technical-parameters

20   Blitzer, L., *Handbook of orbital perturbations*. (Tucson, A Z: University of Arizona) (1970).

21   Alamdari, N., Perturbations in orbital elements of a low earth orbiting satellite. *J. Earth Sp. Phys.,* 33 (2007) 1–12.

22   Flohrer, C., Mutual validation of satellite-geodetic techniques and its impact on GNSS orbit modeling. *Geodätisch-geophys ikalische Arbeiten in der Schweiz.,* 75 (2008) ISBN: 978-3-908440-19-2.

23   Parkinson, B. W. & Spilker, J. J., Global Positioning System: Theory and Applications. *Progress in Astronautics and Aeronautics*, 1, (American Institute of Aeronautics and Astronautics, 1996). doi:10.2514/4.866388

24   Montenbruck, O., Steigenberger, P. & Riley, S., IRNSS Orbit Determination and Broadcast Ephemeris Assessment. In: *Institute of Navigation International Technical Meeting 2015.* (2015) 185–193. ISBN:9781510800434

25   Torre, A. D. & Caporali, A., An analysis of intersystem biases for multi-GNSS positioning. *GPS Solut.*, 19 (2015) 297–307. doi:10.1007/s10291-014-0388-2

26   GPS Navstar, Global Positioning System standard positioning service signal specification. *Report*, 2nd edition (1995) pp 46.

27   Langley, R. B., The orbits of GPS satellites. *GPS World,* 3 (1991) 50–53.

28   Ogaja, C., Applied GPS for Engineers and Project Managers. (2011) pp. 222. ISBN:9781420051124

29   Li, H., Geostationary Satellites Collocation. (Springer Berlin Heidelberg) (2014) pp. 334. ISBN: 978-3-642-40798-7

30   Hugentobler, U. & Montenbruck, O., Satellite Orbits and Attitude. In: *Springer Handbook of Global Navigation Satellite Systems*, edited by Teunissen, P., Montenbruck, O. (Springer International Publishing AG 2017, Cham) (2017) 59–90. doi:10.1007/978-3-319-42928-1_3